Supplement of Atmos. Chem. Phys., 19, 7279–7295, 2019
https://doi.org/10.5194/acp-19-7279-2019-supplement

Supplement of

Development of a versatile source apportionment analysis based on positive matrix factorization: a case study of the seasonal variation of organic aerosol sources in Estonia

Athanasia Vlachou et al.

Correspondence to: André S. H. Prévôt (andre.prevot@psi.ch) and Imad El Haddad (imad.el-haddad@psi.ch)

Table S1. Dates per site.

KJ	Tallinn	Tartu	KJ	Tallinn	Tartu
2013			**2014**		
31.08.2013					03.01.2014
	05.09.2013	05.09.2013		05.01.2014	
08.09.2013	08.09.2013		06.01.2014		
		09.09.2013			07.01.2014
	12.09.2013			11.01.2014	
	13.09.2013			19.01.2014	19.01.2014
	16.09.2013		22.01.2014		
		17.09.2013		26.01.2014	
20.09.2013	20.09.2013			02.02.2014	
	22.09.2013				27.01.2014
		29.09.2013	03.02.2014	03.02.2014	
	30.09.2013			06.02.2014	
02.10.2013				07.02.2014	
	07.10.2013				08.02.2014
	10.10.2013			09.02.2014	
		11.10.2013	11.02.2014		
14.10.2013	14.10.2013		15.02.2014		
18.10.2013				16.02.2014	
	21.10.2013				20.02.2014
		23.10.2013		23.02.2014	
26.10.2013					24.02.2014
	27.10.2013	27.10.2013	27.02.2014		
	04.11.2013			28.02.2014	
07.11.2013				01.03.2014	
		08.11.2013		02.03.2014	
	10.11.2013				04.03.2014
	17.11.2013				08.03.2014
19.11.2013				10.03.2014	
		20.11.2013	11.03.2014		
23.11.2013					16.03.2014
	24.11.2013			17.03.2014	
		28.11.2013			20.03.2014
01.12.2013	01.12.2013			22.03.2014	
			23.03.2014		
	08.12.2013			27.03.2014	
13.12.2013					28.03.2014
		14.12.2013		30.03.2014	
	16.12.2013		31.03.2014		
17.12.2013			04.04.2014		
	23.12.2013			06.04.2014	
	26.12.2013	26.12.2013			09.04.2014
29.12.2013				13.04.2014	
	30.12.2013		16.04.2014		
				20.04.2014	
					21.04.2014
				25.04.2014	25.04.2014
			28.04.2014		

		03.05.2014	03.05.2014
	06.05.2014		
		11.05.2014	
	12.05.2014		
			15.05.2014
		23.05.2014	23.05.2014
	24.05.2014	24.05.2014	
		25.05.2014	
			27.05.2014
		29.05.2014	
		01.06.2014	
			04.06.2014
	05.06.2014	05.06.2014	
		06.06.2014	
		08.06.2014	
		15.06.2014	
			16.06.2014
	17.06.2014		
			20.06.2014
		22.06.2014	
			28.06.2014
	29.06.2014	29.06.2014	
	07.07.2014	07.07.2014	
			10.07.2014
	12.07.2014		
		14.07.2014	
	20.07.2014		
			22.07.2014
		25.07.2014	
		28.07.2014	
		31.07.2014	
	01.08.2014		
			03.08.2014
		04.08.2014	
	05.08.2014		
			07.08.2014
		11.08.2014	
	13.08.2014		
			15.08.2014
		18.08.2014	
		24.08.2014	
	25.08.2014		
			27.08.2014
			31.08.2014
		01.09.2014	

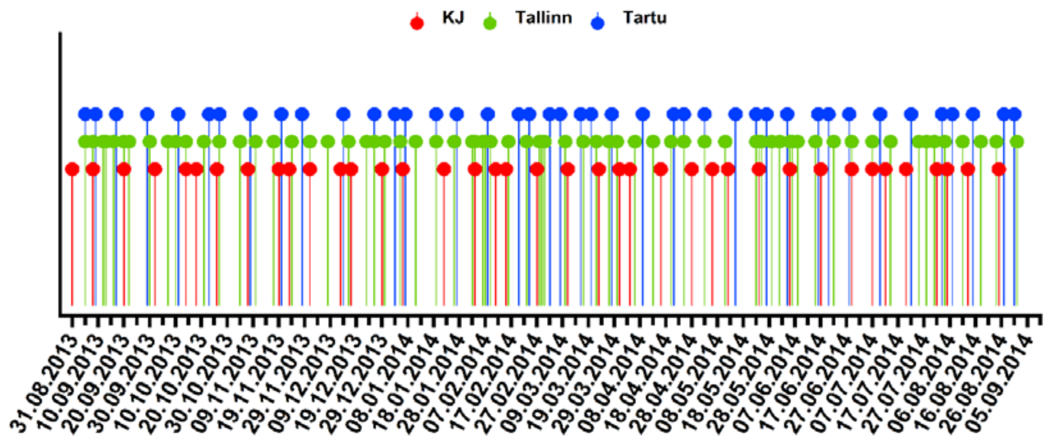

Figure S1. Dates per site. KJ represented in red, Tallinn in green and Tartu in blue.

Table S2. Number of samples per season per site.

	Number of samples per season		
Seasons	**KJ**	**Tallinn**	**Tartu**
Summer	11	16	11
Autumn	9	18	10
Winter	10	18	9
Spring	9	17	12

Table S3. Percentages of true positive and true negative values (accuracy) per factor and the probabilities of false positive and false negative values (probability) for the “ts” method.

	Accuracy		**Probability**	
Time Series	*True Positive*	*True Negative*	*False Positive*	*False Negative*
BBOA	98%	54%	20%	8%
PBOA	91%	100%	0%	53%
WOOA	99%	17%	3%	50%
SOOA	100%	0%	16%	0%

Table S4. Percentages of true positive and true negative values (accuracy) per factor and the probabilities of false positive and false negative values (probability) for the “pr” method.

	Accuracy		**Probability**	
Profiles	True Positive	True Negative	False Positive	False Negative
BBOA	87%	68%	20%	21%
PBOA	91%	100%	0%	56%
WOOA	92%	0%	1%	100%
SOOA	96%	17%	11%	67%

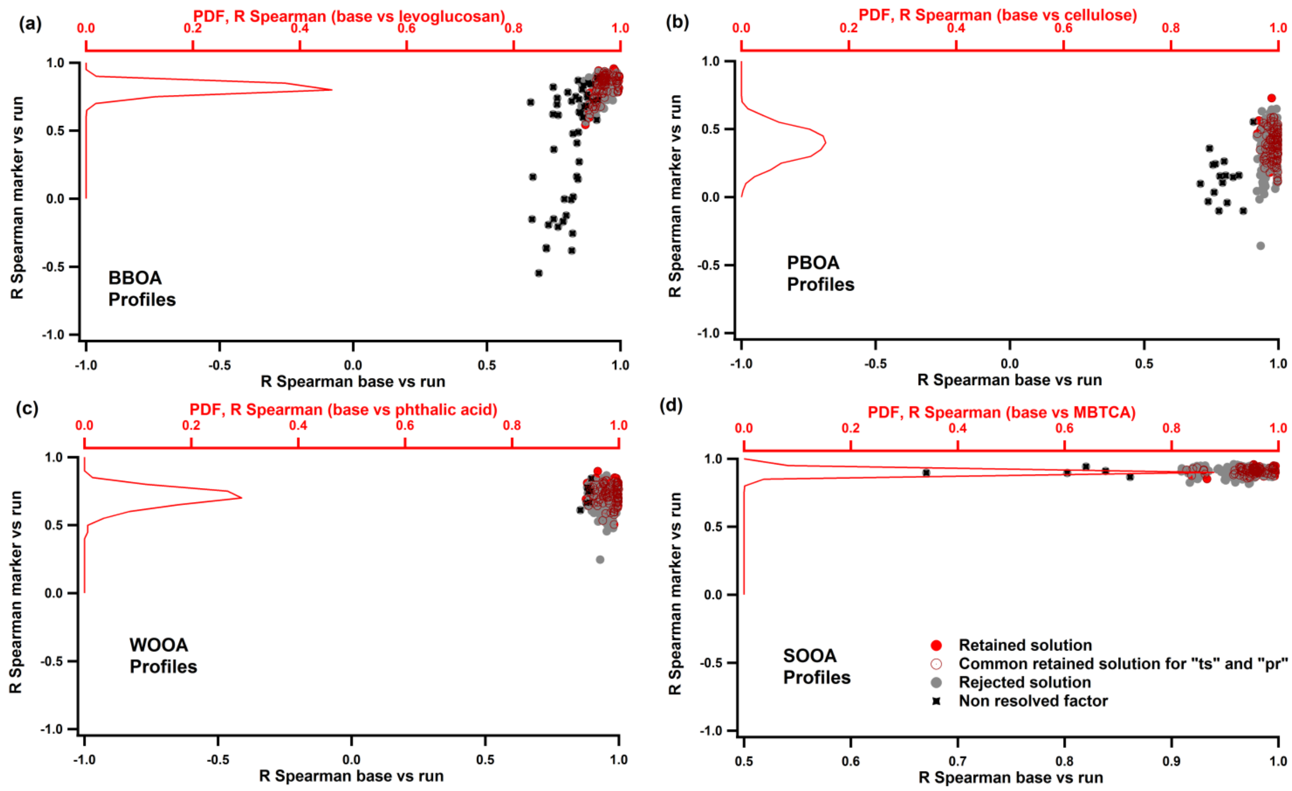

Figure S2. Solution space per factor defined by investigation of the correlation (*R*s) between base case factor profiles and bootstrap run (bottom x-axis) and external marker and bootstrap run (y-axis): BBOA with levoglucosan (a), PBOA with cellulose (b), WOOA with phthalic acid (c) and SOOA with MBTCA (d). The retained solutions are indicated in red and the rejected ones in grey. The points in black represent the runs where the specific factor was not resolved at all. Each PDF (top x-axis) includes the range of *R*s of the correlation between the time series of each base case factor with its respective marker.

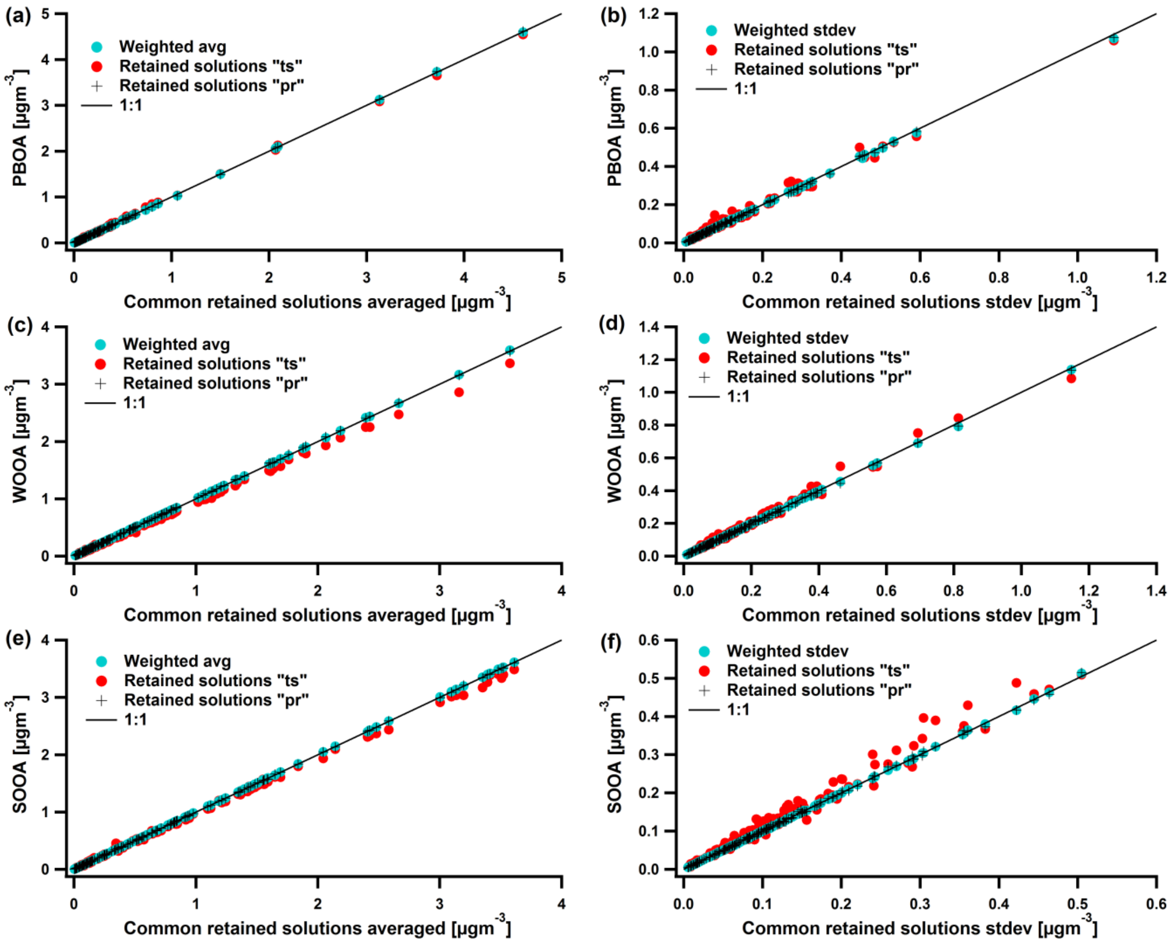

Fig. S3. Scatter plots between factor OA time series averaged (avg) over the common solutions coming from the time series ("ts") and profile ("pr") sorting method plotted in the x-axis, and plotted in the y-axis the factor OA time series averaged over the solutions coming from the "ts" method in red, from the "pr" in black cross and from the weighted average based on the marker, in blue: PBOA and cellulose (a), WOOA and phthalic acid (c) and SOOA and MBTCA (e). The respective scatter plot for the standard deviation (stdev) is shown in (b), (d) and (f).

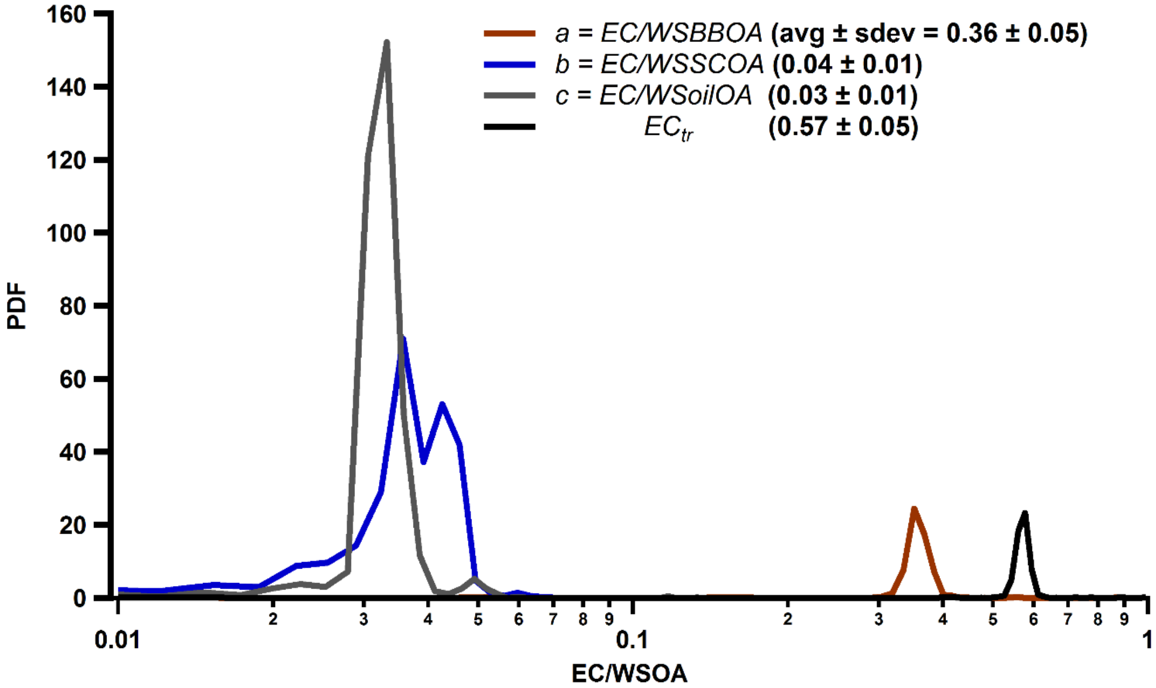

Figure S4. Probability density functions for the EC:WSOA ratios (*a* for WSBBOA, *b* for WSSCOA and *c* for WSoilOA) characteristic of the emissions from the same sources obtained by the 1000 PMF runs.

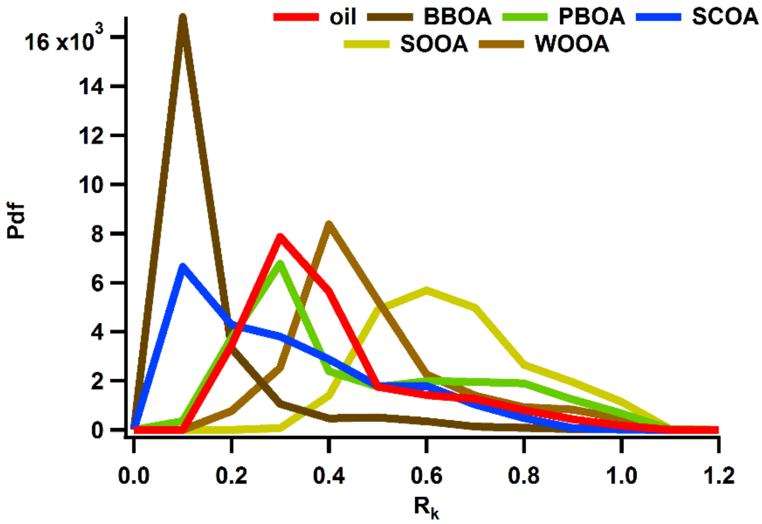

Figure S5. Probability density functions of the recoveries of each factor: oil in red, BBOA in dark brown, PBOA in green, SCOA in blue, SOOA in yellow and WOOA in light brown.

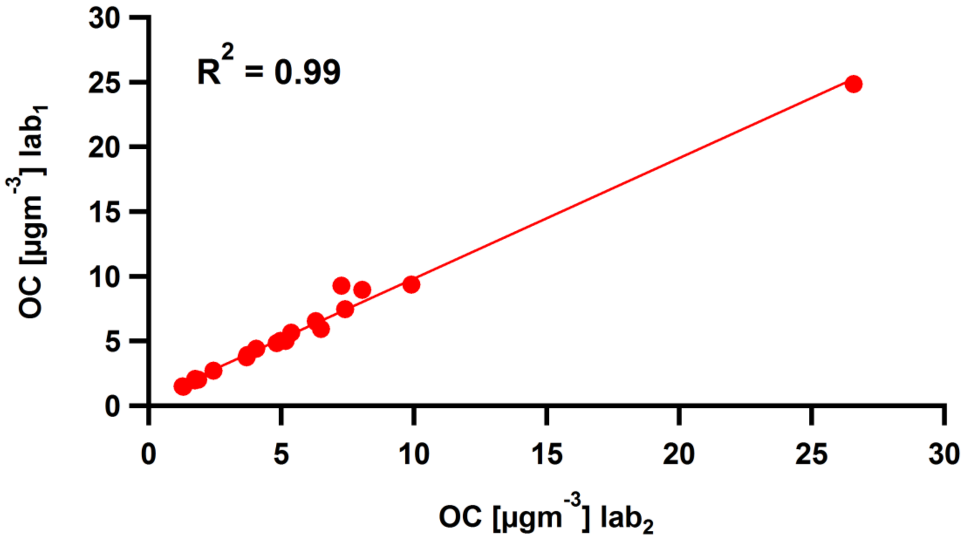

Figure S6. Correlation between OC measured in Bern (lab_1: MICADAS lab, University of Bern) and OC measured in Grenoble (lab_2: Université Grenoble Alpes).

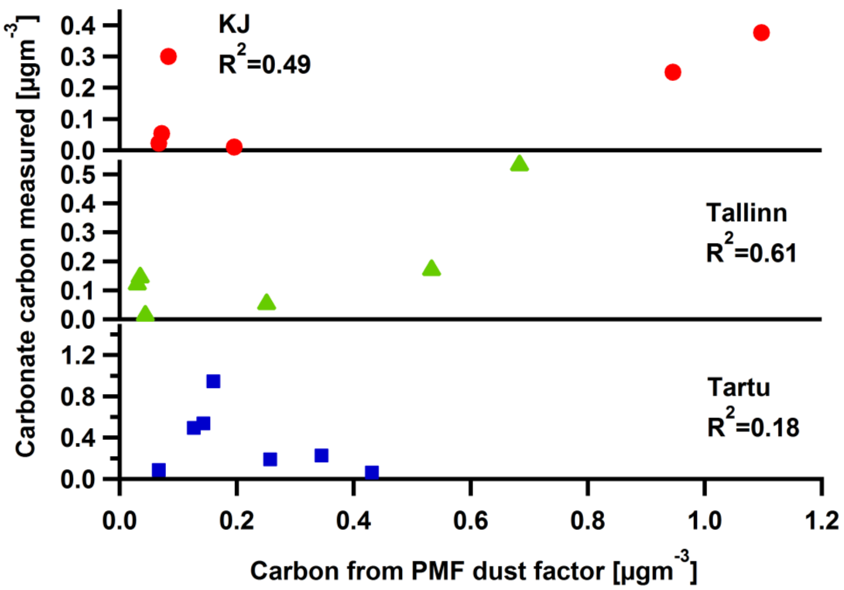

Figure S7. Correlations between carbonate carbon measured and modelled for each site.

Carbonate carbon calculation

In order to estimate the contribution of the carbonate carbon (C_CO_3) in the inorganic dust factor, we calculated the fraction of C_CO_3 (f_{C_CO3}) based on Eq. S1:

$$f_{C\_CO3,i} = \frac{f_{Dust\_PMF}}{\sum_{i=1}^{6} WSOC_i/\left(\frac{OM}{OC}\right)i + f_{Dust\_PMF}/\left(\frac{OM}{OC}\right)Dust} \qquad \text{(S1)}$$

where i indicates the factor (6 OA factors) and f_{Dust_PMF} the fraction of the PMF identified, inorganic dust factor:

$$f_{Dust\_PMF} = \frac{Dust\_PMF * RIE_{CO_3}}{\sum_{i=1}^{6} OAi * RIEorg + Dust\_PMF * RIE_{CO_3}} \qquad \text{(S2)}$$

with OA*i* representing the organic aerosol factor concentrations, Dust_PMF the concentration of the inorganic dust factor as obtained from PMF, $RIEorg$ and RIE_{CO_3} the relative ionisation efficiency of the organics (1.4, Canagaratna et al., 2007) and carbonate (1.16, Bozzetti et al., 2017) respectively.

Finally, we multiplied all water soluble OC (WSOC) factors by the ratio 1 / (1- $f_{C\_CO3,i}$) to rescale the sum of the 6 WSOC factor concentrations to the externally measured WSOC, given that the dust factor is inorganic.

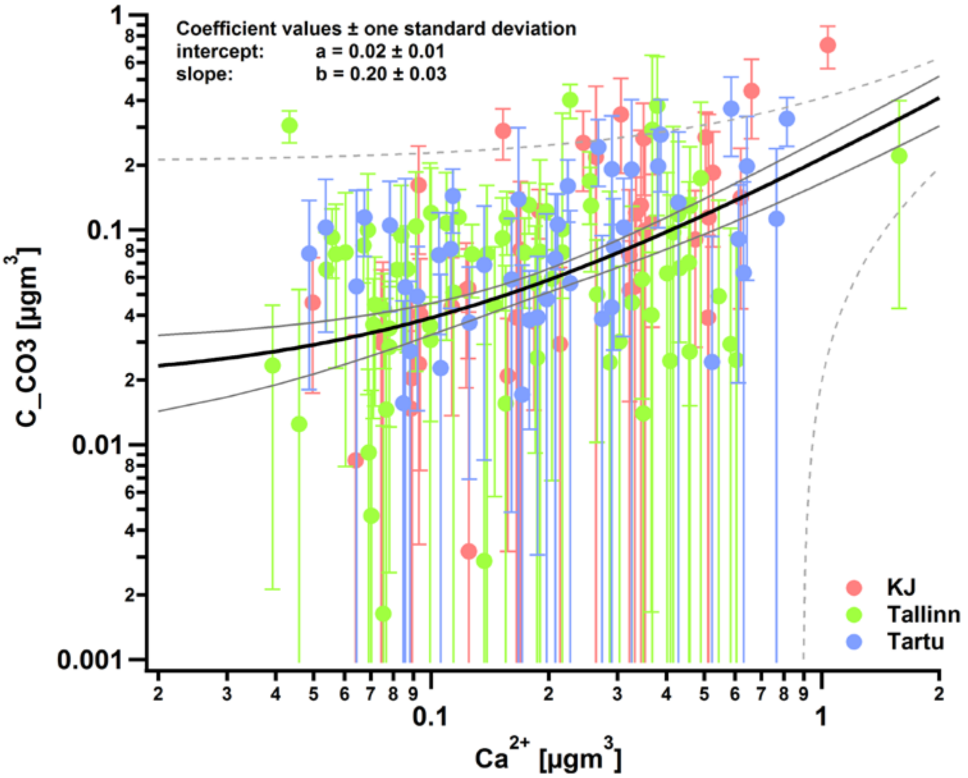

Figure S8. Scatter plot in logarithmic scale between calculated carbonate carbon (C_CO_3) and Ca^{2+}. The black solid line indicates the linear regression, the grey solid lines the confidence bands and the grey dashed lines the predicted bands. Red represents KJ, green Tallinn and blue Tartu.

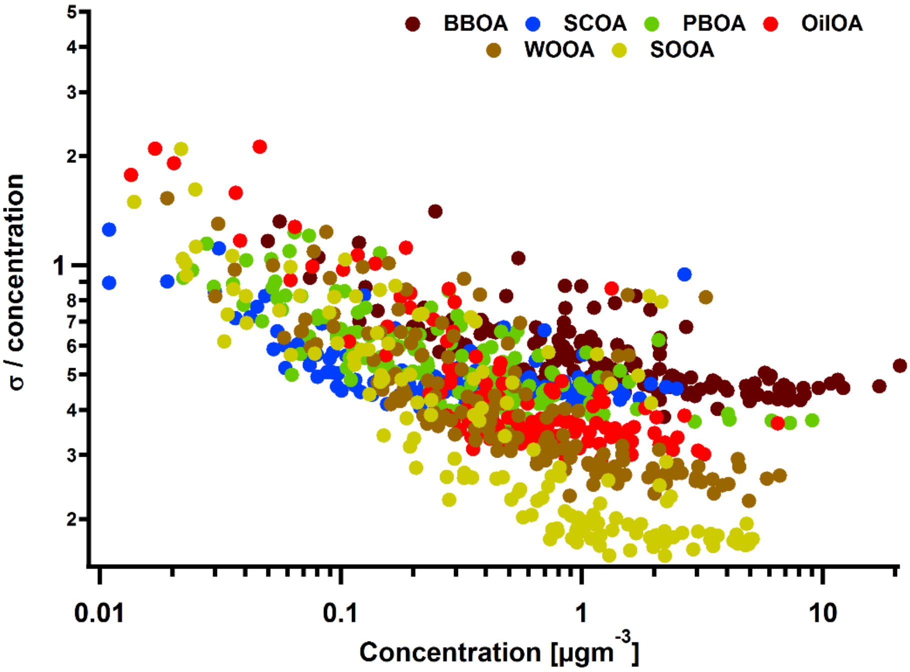

Figure S9. Concentration uncertainties σ for each PMF factor as a function of factor concentration.

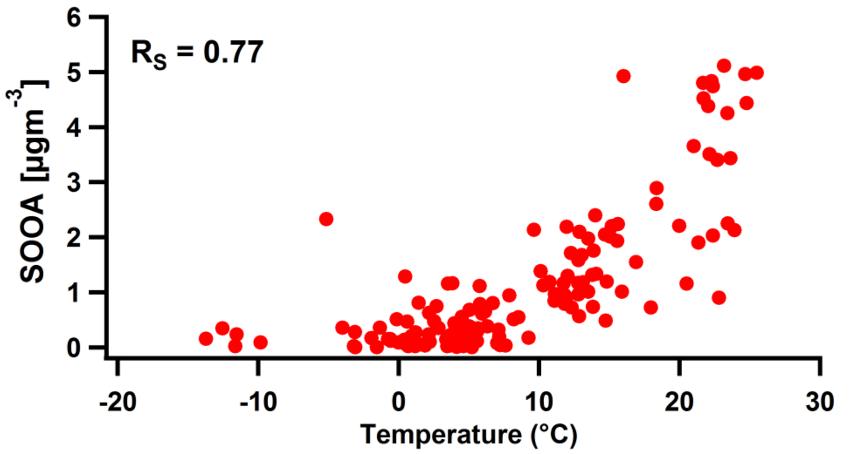

Figure S10. Exponential dependency of SOOA on temperature. The scatter plot includes all sites.

Table S5. OA concentrations per factor per season, with uncertainties.

Factor	Autumn (μgm^{-3})			Winter (μgm^{-3})			Spring (μgm^{-3})			Summer (μgm^{-3})		
	KJ	Tallinn	Tartu	KJ	Tallinn	Tartu	KJ	Tallinn	Tartu	KJ	Tallinn	Tartu
BBOA	1.1±0.7	1.2±0.9	3.8±1.9	1.3±0.8	3.7±2.7	8.4±3.9	0.3±0.3	2.3±1.6	4.0±3.5	1.2±1.0	0.9±0.6	1.6±0.8
SCOA	0.2±0.1	0.5±0.3	0.3±0.2	0.3±0.2	0.7±0.4	0.2±0.1	0.3±0.2	0.6±0.4	0.4±0.3	0.8±0.5	0.5±0.3	0.4±0.2
PBOA	0.1±0.1	0.3±0.2	0.7±0.3	0.1±0.1	0.3±0.2	0.9±0.5	0.2±0.2	1.2±0.8	2.1±1.3	0.4±0.2	0.4±0.2	0.5±0.2
Oil OA	0.7±0.3	0.4±0.3	0.3±0.2	0.4±0.2	0.6±0.2	0.2±0.1	1.4±0.9	0.8±0.3	0.7±0.4	1.4±0.5	1.0±0.4	0.9±0.3
WOOA	1.6±0.5	0.6±0.4	1.3±0.5	1.4±0.5	2.2±0.8	1.5±0.5	0.3±0.1	1.0±0.4	0.6±0.3	0.8±0.5	0.5±0.2	0.2±0.1
SOOA	0.3±0.1	1.1±0.4	0.9±0.2	0.1±0.1	0.3±0.2	0.2±0.2	0.7±0.2	1.4±0.4	0.9±0.3	1.8±0.7	2.8±0.6	2.1±0.4

Table S6. Relative contributions per factor per season to the OA, with uncertainties.

Factor	Autumn (%)			Winter (%)			Spring (%)			Summer (%)		
	KJ	Tallinn	Tartu	KJ	Tallinn	Tartu	KJ	Tallinn	Tartu	KJ	Tallinn	Tartu
BBOA	24±18	27±13	53±14	30±19	39±16	73±21	14±11	30±14	47±18	18±12	17±12	30±16
SCOA	4±2	16±5	4±1	13±5	18±6	2±1	16±5	12±4	5±2	13±3	10±3	7±2
PBOA	3±2	7±3	9±5	3±2	3±2	9±6	7±4	11±5	21±8	6±3	7±3	9±4
Oil OA	16±5	13±4	4±2	15±6	11±5	1±1	36±14	14±5	8±3	26±7	16±5	15±4
WOOA	39±13	13±5	16±6	36±14	25±9	13±5	13±6	15±7	9±5	11±4	9±4	4±3
SOOA	14±5	24±5	13±3	4±2	3±2	2±1	14±5	18±5	11±3	26±5	41±7	35±7

References

Bozzetti, C., El Haddad, I., Salameh, D., Daellenbach, K. R., Fermo, P., Gonzalez, R., Minguillón, M. C., Iinuma, Y., Poulain, L., Elser, M., Müller, E., Slowik, J. G., Jaffrezo, J.-L., Baltensperger, U., Marchand, N., Prévôt, A. S. H.: Organic aerosol source apportionment by offline-AMS over a full year in Marseille, Atmos. Chem. Phys., 17, 8247-8268, doi:10.5194/acp-17-8247-2017, 2017b.

Canagaratna, M. R., Jayne, J. T., Jimenez, J. L., Allan, J. D., Alfarra, M. R., Zhang, Q., Onasch, T. B., Drewnick, F., Coe, H., Middlebrook, A., Delia, A., Williams, L. R., Trimborn, A. M., Northway, M. J., DeCarlo, P. F., Kolb, C. E., Davidovits, P. and Worsnop, D. R.: Chemical and microphysical characterization of ambient aerosols with the Aerodyne aerosol mass spectrometer, Mass Spectrom. Rev., 26, 185-222, doi:10.1002/mas.20115, 2007.